BIOCHEMISTRY
including biophysical chemistry & molecular biology

ARTICLE

pubs.acs.org/biochemistry

Conferment of Folding Ability to a Naturally Unfolded Apocytochrome *c* through Introduction of Hydrophobic Amino Acid Residues

Masaru Yamanaka, Misa Masanari, and Yoshihiro Sambongi*

Graduate School of Biosphere Science, Hiroshima University, 1-4-4 Kagamiyama, Higashi-Hiroshima, Hiroshima 739-8528, Japan

ABSTRACT: Hyperthermophilic *Aquifex aeolicus* cytochrome c_{555} (AA c_{555}) exceptionally folds even in the apo state, unlike general cytochromes *c* including mesophilic *Pseudomonas aeruginosa* cytochrome c_{551} (PA c_{551}), which is structurally homologous to AA c_{555} in the holo state. Here we hypothesized that the exceptional apo AA c_{555} folding can be attributed to nine hydrophobic amino acid residues and proved this using a PA c_{551} variant (denoted as PA-nh) carrying the *n*ine *h*ydrophobic residues at structurally corresponding positions. Circular dichroism experiments showed that the apo PA-nh variant became folded, unlike the wild-type apo PA c_{551}, and exhibited much higher stability than the wild type. Another difference between the holo forms of AA c_{555} and PA c_{551} is the existence of an extra helix in the former. Introduction of the amino acid residues forming the extra helix of AA c_{555} into the PA-nh variant did not significantly affect its folding ability in the apo state. Therefore, the nine hydrophobic residues introduced into the apo PA-nh variant were enough to confer the folding ability. PA c_{551} represents the first example of the conversion of an intrinsically unfolded apocytochrome *c* into an autonomously folded one, which was revealed by means of a protein engineering method without heme. Although heme is generally considered to be a trigger of apocytochrome *c* folding, the present results demonstrate a new heme-independent folding mechanism.

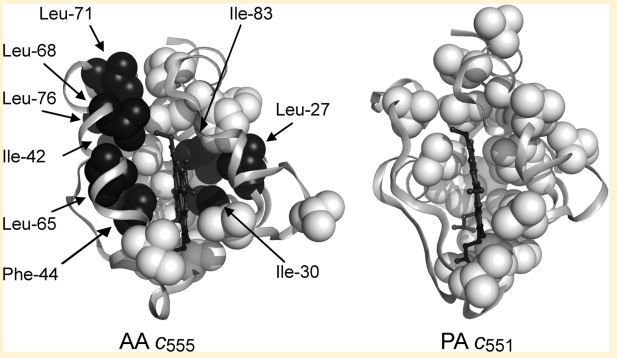

Monoheme soluble cytochromes *c* are small proteins that function as electron carriers in the cell. Cytochromes *c* are helical proteins and are characterized by covalently bound cofactor heme in the conserved Cys-Xxx-Xxx-Cys-His (CXXCH) motif. The heme occupies the majority of the interior hydrophobic core of the holocytochrome *c* structure.

Using several mesophilic cytochromes *c*, such as horse heart mitochondrial cytochrome *c*, *Paracoccus denitrificans* cytochrome c_{550}, and *Pseudomonas aeruginosa* cytochrome c_{551} (PA c_{551}), the effect of heme on protein folding has been investigated.[1−6] Removal of heme from these cytochromes *c* results in loss of the helical structure. Unlike mesophilic cytochromes *c*, thermophilic *Hydrogenobacter thermophilus* cytochrome c_{552} (HT c_{552}) has a partially folded structure in its apo state.[7] Despite this difference between these mesophilic and thermophilic apocytochromes *c*, heme binding to these apoproteins, in common, induces helical structure formation. Such helix formation after heme binding leads to cytochrome *c* folding, followed by stable structure formation allowing biological functions.

In contrast to the general understanding of cytochrome *c* folding after the heme binding, it was recently shown that hyperthermophilic *Aquifex aeolicus* cytochrome c_{555} (AA c_{555}) can exceptionally form a helical structure to the same extent in the apo state as in its holo form.[6] Circular dichroism (CD) and visible spectral analyses demonstrated that the C12A/C15A variant of AA c_{555}, which has mutations in the CXXCH motif and cannot covalently bind heme, forms the helical structure even in the apo state. For convenience, the apo AA c_{555} C12A/C15A variant is denoted simply as "apo AA c_{555}" in this paper.

In order to gain a structural insight into the exceptional folding ability of AA c_{555}, X-ray crystallographic analysis has been carried out on its holo form.[8] The three-dimensional main chain structure of holo AA c_{555} is the most superimposable on those of homologous class ID monoheme cytochromes *c* including PA c_{551}. Therefore, it would be an appropriate experimental strategy to introduce AA c_{555} residues into the PA c_{551} background in order to examine any specific amino acid residues as to their effects on folding ability. However, this has not been carried out yet.

In the present study, we carefully compared the three-dimensional structures of the holo forms of AA c_{555} and PA c_{551}. As a result, several amino acid residues were selected as key candidate residues for the folding ability of apo AA c_{555} without heme. These residues were introduced at the structurally corresponding positions in PA c_{551}, and the resulting PA c_{551}variants were examined as to their folding ability.

Received: October 14, 2010
Revised: February 17, 2011
Published: February 17, 2011

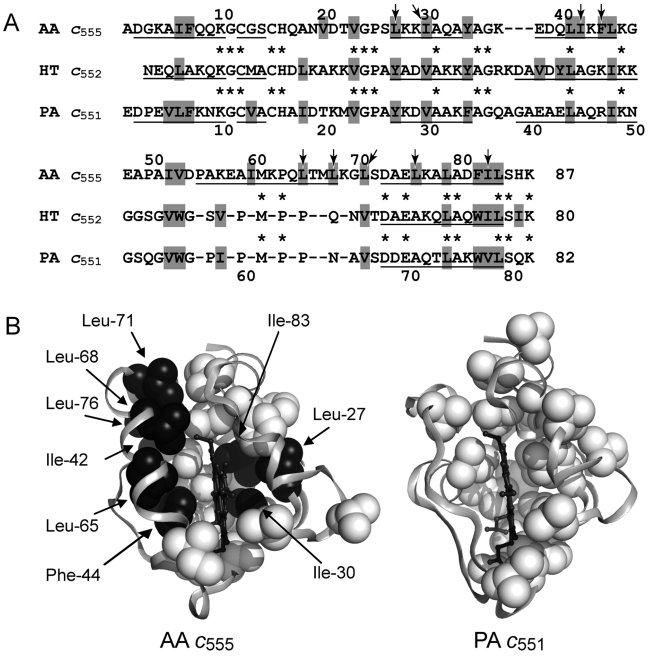

Figure 1. Structure comparison and contrast. (A) Sequence alignment of AA c_{555}, PA c_{551}, and HT c_{552}. The amino acid sequences of the three proteins are aligned so that the structurally corresponding residues in the three-dimensional structures match. Gaps in the alignment are indicated by dashes. Identical residues in the three proteins are indicated by asterisks between the sequences. Hydrophobic residues, Leu, Ile, Phe, Trp, Tyr, and Val, are highlighted in gray. Residues forming the helix structure are underlined. The nine characteristic hydrophobic residues, which seem to be responsible for the folding ability of apo AA c_{555}, are indicated by arrows. (B) Three-dimensional structures of AA c_{555} and PA c_{551}. The main chain backbone and heme are depicted as ribbon and stick-and-ball models, respectively. The side chains of hydrophobic residues, Leu, Ile, Phe, Trp, Tyr, and Val, are depicted as a space-filling model, and among them the nine characteristic hydrophobic residues are indicated by arrows.

MATERIALS AND METHODS

Three-Dimensional Structure Comparison. The three-dimensional structures of AA c_{555} and PA c_{551} were compared by using the molecular graphics program PyMOL.[9] The structural information was taken from PDB code 2zxy for AA c_{555} and 351c for PA c_{551}. The backbone structures of the two proteins including their heme groups were superimposed, and characteristic amino acid residues of AA c_{555} were selected.

Strains and Plasmids. *Escherichia coli* strain JCB387 was used to produce the PA c_{551} wild type and its variants.[10] *E. coli* strain DH5α was used for routine gene engineering. Plasmid pKPA1 was used for the production of the PA c_{551} wild type.[11] Nine residues, Tyr-27, Val-30, Ala-45, Arg-47, Pro-63, Asn-64, Val-66, Ala-71, and Val-78, in PA c_{551} were substituted with Leu-27, Ile-30, Ile-42, Phe-44, Leu-65, Leu-68, Leu-71, Leu-76, and Ile-83, respectively, which are the structurally corresponding nine hydrophobic residues in AA c_{555} (Figure 1A) to obtain the PA-nh variant ("nh" stands for *n*ine *h*ydrophobic). PrimeSTAR Max DNA polymerase (TaKaRa Bio) was used for the four steps of inverse PCR involving plasmid pKPA3,[11] carrying the V78I mutation of PA c_{551}, as a template DNA. The resulting plasmid was denoted as pKPA17, which encodes the PA-nh variant.

To introduce the amino acid residues forming the extra helix of AA c_{555} (Figure 1A) into the PA-nh variant, two further steps of inverse PCR were performed for pKPA17 to generate plasmid pKPA18, which encodes the PA-nh/eh variant ("eh" stands for *e*xtra *h*elix). Specifically, the stretch of Gly-57 to Ala-65 in the PA-nh variant was substituted with that of Asp-54 to Gly-70 in AA c_{555} (Figure 1A). Each plasmid carrying the cytochrome *c* gene confers resistance to ampicillin. Plasmid pEC86 was used for coexpression of the *E. coli* cytochrome *c* maturation proteins (CcmABCDEFGH)[12] for efficient production of cytochromes *c*. Plasmid pEC86 confers resistance to chloramphenicol.

Preparation of Holo PA c_{551} Wild Type, PA-nh, and PA-nh/eh. *E. coli* strain JCB387 transformed with pEC86 and pKPA1, pKPA17, or pKPA18 was initially grown in liquid LB medium containing 100 μg/mL ampicillin and 34 μg/mL chloramphenicol. These LB precultures (20 mL) were each inoculated into 2 L of minimal medium in a 5 L flask as described previously.[6] Cells were grown at 37 °C with shaking for 24 h before harvesting. Periplasmic extracts were obtained by the cold osmotic shock method as described previously.[13] The periplasmic extracts were dialyzed against 10 mM Tris-HCl (pH 8.0) and then loaded onto a HiTrap Q column (GE Healthcare) that had been equilibrated with the same buffer. The cytochrome *c* fractions were eluted with 10 mM Tris-HCl (pH 8.0) containing a NaCl concentration gradient (0−500 mM) and then dialyzed against 25 mM sodium acetate buffer (pH 5.0). The fractions were further loaded onto a HiTrap SP column (GE Healthcare) that had been equilibrated with the same buffer. The cytochrome *c* fractions were eluted with 25 mM sodium acetate buffer (pH 5.0) containing a NaCl concentration gradient (0−500 mM), followed by loading onto a Superdex 75 gel filtration column (GE Healthcare) equilibrated and eluted with 25 mM sodium acetate buffer (pH 5.0). Protein concentrations were determined spectrophotometrically using the extinction coefficient at 205 nm due to the peptide bond.[14]

Preparation of the Apo PA c_{551} Wild Type, PA-nh, and PA-nh/eh. The apo forms of the PA c_{551} wild type and its variants were prepared by the modified method of Fisher et al.[2] Ten milligrams of Ag_2SO_4 in 0.1 mL of ultrapure water and 80 μL of acetic acid was added to 0.8 mL of 0.3−0.5 mM purified holocytochrome *c* solution. The solutions were incubated in the dark for 4 h at 50 °C and then centrifuged for 20 min at 15000*g* to remove heme aggregates precipitated. The supernatants were loaded onto a PD-10 desalting column (GE Healthcare) equilibrated with 25 mM sodium acetate buffer (pH 5.0), and proteins were eluted with the same buffer. To dissociate their silver mercaptide bonds, the proteins were treated with 6 M guanidine hydrochloride and 1 M dithiothreitol (DTT). The solutions were incubated in the dark for 2 h at 25 °C and then centrifuged for 20 min at 15000*g* to remove the silver mercaptide of DTT. The clear supernatants were loaded onto a PD-10 column equilibrated with 25 mM sodium acetate buffer (pH 5.0), and apocytochromes *c* were eluted with the same buffer. Confirmation of the absence of residual holoproteins was achieved by means of visible absorption spectra and SDS−PAGE followed by heme staining. Protein concentrations were determined spectrophotometrically using the extinction coefficient at 205 nm.

Visible Absorption and Circular Dichroism Spectroscopies. Visible absorption spectra (400−600 nm) of the purified holocytochromes *c* (9 μM) in 20 mM potassium phosphate buffer (pH 7.2) were obtained with a JASCO V-530 spectrophotometer (JASCO) at 25 °C. Samples were reduced by the

addition of a few grains of disodium dithionite. Pyridine ferrohemochromes of these proteins were prepared,[15] and their visible absorption spectra (400−600 nm) were obtained similarly. To investigate the 695 nm peak due to the Fe−S coordination bond of the oxidized cytochromes *c*, visible absorption spectra (650−750 nm) of the purified holocytochromes *c* (200 μM) in 20 mM potassium phosphate buffer (pH 7.2) in the presence of 10 mM potassium ferricyanide were obtained similarly to that described previously.[16] Circular dichroism (CD) spectra of the holo- and apocytochromes *c* (20 μM) in 20 mM potassium phosphate buffer (pH 7.2) were obtained with a JASCO J-820 spectrometer (JASCO) at 25 °C.

Electrochemical Measurements of Holocytochromes *c*. The electrochemical properties of the purified holocytochromes *c* were analyzed by the cyclic voltammetry (CV) method. CV experiments were performed with a Potentiostat Autolab PGSTAT 12 (Eco Chemie), similarly to our previous study.[17] A glassy carbon electrode (GCE) was polished with a 0.05 μm alumina slurry. The protein solutions (2 μL, about 0.5 mM) in 20 mM sodium acetate buffer (pH 5.0) were spread evenly with a microsyringe over the surface of the GCE. Then the GCE surface was covered with a semipermeable membrane. An Ag|AgCl electrode in a saturated NaCl solution and a Pt wire were employed as the reference and counter electrodes, respectively. The potential sweep range was +400 to −400 mV vs the Ag|AgCl electrode in the saturated NaCl solution with a scan rate of 20 mV/s. All of the experiments were performed at 25 °C under an N_2 atmosphere. From the observed redox potentials (E), midpoint redox potential (E_m) values relative to the standard hydrogen electrode (SHE) were determined from the averages of the reductive and oxidative peak potentials.

Thermal Stability Measurement. Thermal denaturation experiments were carried out by obtaining CD spectra in a pressure-proof cell compartment (JASCO) attached to a JASCO J-820 CD spectrometer.[18,19] Solutions of air-oxidized holo and apo PA c_{551} wild type, PA-nh, and PA-nh/eh (20 μM) in 20 mM sodium acetate buffer (pH 5.0) were subjected to analysis. The temperature-dependent CD ellipticity change at 222 nm was monitored in a cuvette of 1 mm path length. The CD values were recorded from 30 to 150 °C or 10 to 90 °C at temperature intervals of 1 °C and a heating rate of 1.0 °C/min. The raw data were subjected to nonlinear least-squares fitting with MATHEMATICA 3.0 as described previously.[20]

The temperature of the midpoint of the transition (T_m) and the enthalpy change during protein denaturation at T_m (ΔH_m) were calculated through curve fitting of the resulting CD values versus the temperature by van't Hoff analysis. The fitting curves obtained in the temperature range of −40 to +40 of T_m were used to calculate thermodynamic parameters in order to precisely reflect protein denaturation. The entropy change during protein denaturation at T_m (ΔS_m) was calculated using the equation $\Delta S_m = \Delta H_m/T_m$.

Because the apo PA c_{551} wild type exhibited no transition with the temperature increase from 10 to 90 °C (see Figure 3A), its thermodynamic parameters could not be determined. Therefore, thermodynamic parameters cannot be compared between the variants (PA-nh and PA-nh/eh) and the PA c_{551} wild type in their apo states. In contrast, the differences in the free energy changes during protein denaturation between the holo forms of the variants and the PA c_{551} wild type at the wild-type T_m ($\Delta\Delta G_{mut}$) were calculated using the equation given by Becktel and Schellman,[21] $\Delta\Delta G_{mut} = \Delta T_m(\text{mut-wt})\Delta S_m(\text{wt})$, where ΔT_m (mut-wt) is the difference in T_m value between the holo forms of the variants and wild type and ΔS_m(wt) is the entropy change of the holo PA c_{551} wild type at its T_m.

The differences in the free energy changes during protein denaturation between the apo and holo forms of PA-nh, PA-nh/eh, and AA c_{555} at the T_m of each holo form ($\Delta\Delta G_{heme}$) were also calculated as $\Delta\Delta G_{heme} = \Delta T_m(\text{apo-holo})\Delta S_m(\text{holo form})$, where ΔT_m (apo-holo) is the difference in T_m value between the apo- and holoproteins and ΔS_m(holo form) is the entropy change of each holoprotein at its T_m.

RESULTS

Three-Dimensional Structure Comparison between AA c_{555} and the PA c_{551} Wild Type. Our previous study showed that an extra helix containing the heme-liganding Met residue exists in AA c_{555},[8] which is not found in the PA c_{551} and HT c_{552} proteins. In this study, we further realized that nine hydrophobic residues existed specifically in AA c_{555}, i.e., not in PA c_{551} (Figure 1A). These nine hydrophobic residues, Leu-27, Ile-30, Ile-42, Phe-44, Leu-65, Leu-68, Leu-71, Leu-76, and Ile-83, of AA c_{555} are dispersed in four helices including the extra helix, and all face the interior of the protein molecule (Figure 1B). These residues exhibit higher hydrophobicity than the respective structurally corresponding residues of PA c_{551}, Tyr-27, Val-30, Ala-45, Arg-47, Pro-63, Asn-64, Val-66, Ala-71, and Val-78.[22] Among the residues in HT c_{552} corresponding to these nine PA c_{551} amino acids, only Ile-76 is identical to the AA c_{555} residue (Ile-83, Figure 1A). This further indicates the specificity of the nine residues in the AA c_{555} sequence.

The side chains of the nine hydrophobic residues of AA c_{555} spatially interact with neighboring residues and allow more tight packing in the protein interior than in the case of PA c_{551} (Figure 1B). The details are as follows. Leu-27, Ile-30, and Ile-83 of AA c_{555} allow hydrophobic packing together with Phe-7, Leu-41, and Phe-82. The corresponding residues in PA c_{551} are Tyr-27, Val-30, Val-78, Phe-7, Leu-44, and Trp-77, respectively (Figure 1A). Ile-42, Leu-68, Leu-71, and Leu-76 of AA c_{555} also allow hydrophobic packing together with Ile-6, Leu-45, and Leu-79. The corresponding residues in PA c_{551} are Ala-45, Asn-64, Val-66, Ala-71, Leu-6, Ile-48, and Leu-74. Phe-44 and Leu-65 of AA c_{555} interact with heme-liganding Met-61, whereas the corresponding Arg-47, Pro-63, and Met-61 in PA c_{551} do not.

From the three-dimensional structure comparison above, we speculated that the nine hydrophobic residues and extra helix result in the exceptional folding of apo AA c_{555}, because a hydrophobic interaction is a major factor in protein folding [23] and helix formation strengthens a protein structure. In fact, the nine hydrophobic residues and extra helix were necessary for formation of the proper structure of AA c_{555}: mutations of these residues in AA c_{555} resulted in aberrant proteins exhibiting heterogeneity when expressed in *E. coli* (M. Yamanaka, unpublished results).

In order to experimentally prove the effects of the nine hydrophobic residues and extra helix of AA c_{555}, two variants of PA c_{551}, i.e., PA-nh having the nine characteristic hydrophobic residues of AA c_{555} and PA-nh/eh having the amino acid residues forming the extra helix of AA c_{555} in addition to the nine hydrophobic residues, were examined in this study. We also constructed a gene encoding a PA c_{551} variant carrying only the amino acid residues forming the extra helix of AA c_{555}. However, its expression level in *E. coli* was far lower than those of the PA-nh

Table 1. Visible Absorption Spectra Peaks and E_m Values of the Holo Forms of the PA c_{551} Wild Type, PA-nh, and PA-nh/eh[a]

protein	oxidized λ_{max} (nm)	reduced λ_{max} (nm)	pyridine ferrohemochrome α-band λ_{max} (nm)	E_m (mV)
PA c_{551} wild type	408	416	549	+317
	530	521		
	695	551		
PA-nh	399	416	549	+160
		522		
		551		
PA-nh/eh	405	416	549	+134
	525	523		
		552		

[a] The experimental errors of the E_m values are all ±5 mV.

and PA-nh/eh variants. Thus, the PA-nh and PA-nh/eh variants were used in the following experiments.

Visible Absorption Spectra of Holocytochromes *c*. The visible absorption spectra of the holo PA c_{551} wild type, PA-nh, and PA-nh/eh were measured to examine the effects of mutations on the heme environment in the protein interior. The peak wavelengths in the visible absorption spectra of these proteins are listed in Table 1. The visible absorption spectra of the reduced PA c_{551} wild type, PA-nh, and PA-nh/eh showed α-band maxima at 551, 551, and 552 nm, respectively, which were within the range for typical cytochromes *c*. The pyridine ferrohemochromes of these proteins all showed an α-band maximum at 549 nm, suggesting that the heme is covalently bound to these proteins via two thioether bonds formed between the two Cys residues of the CXXCH motif and the two vinyl groups of the heme.[15,24,25]

The oxidized holo PA c_{551} wild type exhibited an absorption peak at 695 nm (Table 1), which is due to the Fe−S coordination bond between the heme iron and heme-liganding Met sulfur atom. However, the oxidized holo forms of PA-nh and PA-nh/eh showed no peak at 650−750 nm in contrast to that of the PA c_{551} wild type, suggesting that heme does not form a coordination linkage with the Met residue in the two variants.

Redox Potentials of Holocytochromes *c*. CV experiments have been performed on the holo forms of the PA c_{551} wild type and PA-nh and PA-nh/eh variants. The resulting E_m values of PA-nh and PA-nh/eh variants were greatly decreased compared with that of the PA c_{551} wild type (Table 1). In cytochrome *c*, an axial Met ligand generally leads to a high redox potential. The decreases in the E_m values of the two variants indicate intramolecular rearrangement in the vicinity of the heme. Together with the visible absorption spectra showing disappearance of the 695 nm peak for the oxidized PA-nh and PA-nh/eh variants, the mutations may cause cleavage of the Fe−S coordination bond between the heme and the heme-liganding Met residue.

Far-UV CD Spectra of Holocytochromes *c*. Far-UV CD spectra (195−260 nm) were obtained to examine the secondary structure formation of the holo forms of PA c_{551} wild type, PA-nh, and PA-nh/eh. The ellipticity peak at 222 nm, representing the helix structure, was observed in the holo forms of these proteins (Figure 2). The helical contents of holo PA c_{551} wild type, PA-nh, and PA-nh/eh were estimated to be 35%, 35%, and 34%, respectively, by means of CD deconvolution, using the K2D algorism.[26,27] These values comparatively exhibit that the helical contents of these three holoproteins are the same. Although the amino acid residues forming the extra helix in AA c_{555} were introduced into the PA-nh/eh variant, the helical content of the variant was not greater than those of the PA c_{551} wild type and PA-nh in their holo states. This indicates that the extra helix found in AA c_{555} is not formed in the holo PA-nh/eh variant or regions of some helices collapse due to the formation of the extra helix. The ellipticity peak height around 208 nm, which is also attributed to the helical structure, differed for the PA c_{551} wild type, PA-nh, and PA-nh/eh (Figure 2). We do not know the structural mechanism underlying this difference, but it may be due to some undefined structural alteration in the holo PA-nh and PA-nh/eh variants upon mutation.

Far-UV CD Spectra of Apocytochromes *c*. In the far-UV CD spectrum of the apo PA c_{551} wild type the ellipticity peaks at 208 and 222 nm had disappeared (Figure 2). In contrast, however, the apo PA-nh and PA-nh/eh variants still exhibited ellipticity peaks at 208 and 222 nm. The helical contents of the apo forms of the PA c_{551} wild type, PA-nh, and PA-nh/eh were estimated to be 9%, 32%, and 55%, respectively, by means of deconvolution.[26,27] These results suggest that apo PA-nh and PA-nh/eh retain the helical structure even upon the removal of the heme. The helical content of apo PA-nh/eh was greater than that of its holo form, suggesting that an additional helix is formed in the apo state compared with in the holo one. One possible reason is that the extra helix found in the holo AA c_{555} structure is only formed in the apo PA-nh/eh variant, i.e., not in its holo form. The other possibility is that some regions of the preexisting helices in the holo PA c_{551} wild type were not able to be formed in the holo PA nh/eh variant due to the introduction of the extra helix.

Effects of Mutations on the Thermal Stability of Holocytochromes *c*. In order to thermodynamically elucidate the effects of mutations on protein structure, thermal denaturation experiments were carried out on the air-oxidized holo PA c_{551} wild type, PA-nh, and PA-nh/eh, with monitoring by CD at 222 nm. For instance, the raw CD data for the holo and apo PA c_{551} wild-type proteins were obtained as a function of temperature (Figure 3A) and showed cooperative denaturation of the holoprotein but not of the apoprotein.

Similar to the PA c_{551} wild type, the holo forms of PA-nh and PA-nh/eh became cooperatively denatured with the temperature increase from 30 to 150 °C (Figure 3). The T_m values of the holo forms of the PA c_{551} wild type, PA-nh, and PA-nh/eh were estimated to be 85.7, 90.5, and 86.5 °C, respectively (Table 2). The $\Delta\Delta G_{mut}$ values of the PA-nh and PA-nh/eh variants, which represent differences in the free energy change during protein denaturation between the holo forms of these variants and the PA c_{551} wild type, were estimated to be 4.6 kJ/mol for PA-nh and 0.8 kJ/mol for PA-nh/eh, respectively (Table 2). These results indicate that the mutations result in structural stabilization in their holo states.

The enthalpy change at T_m(ΔH_m) and entropy change at T_m(ΔS_m) values for the holo PA-nh variant were smaller than those for the holo PA c_{551} wild type (Table 2). In general, upon mutation(s), a decrease in the ΔH_m value leads to protein destabilization, and conversely, a decrease in the ΔS_m value leads to protein stabilization. In comparison with the holo PA c_{551} wild type, therefore, the holo PA-nh variant is destabilized in terms of enthalpy. This may be due to the loss of some preexisting interactions including the Fe−S coordination bond (as shown in Table 1) in the holo PA-nh variant. This enthalpic disadvantage is mitigated by the more favorable entropic effect during

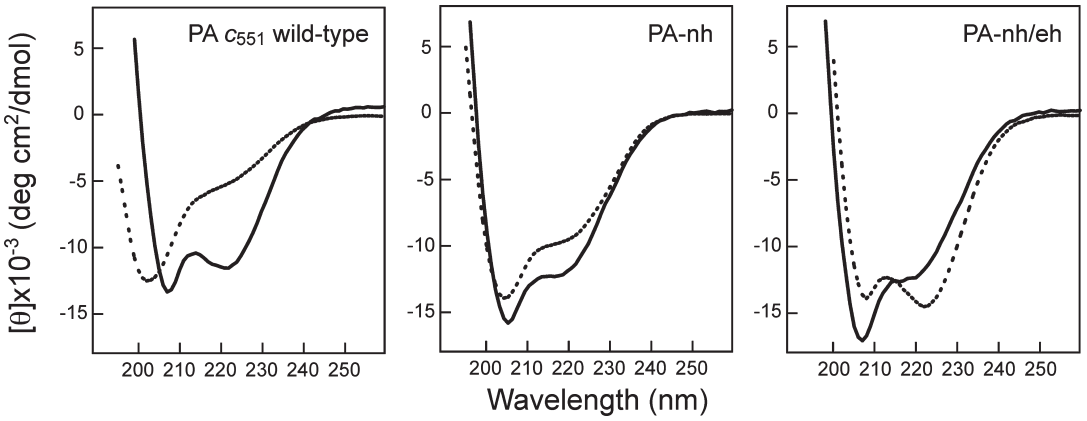

Figure 2. Far-UV CD spectra of the holo and apo forms of cytochromes *c*. Far-UV CD spectra of holo- (solid lines) and apo- (dotted lines) cytochromes *c* are depicted. The data for the PA c_{551} wild type (left), PA-nh variant (center), and PA-nh/eh (right) are shown.

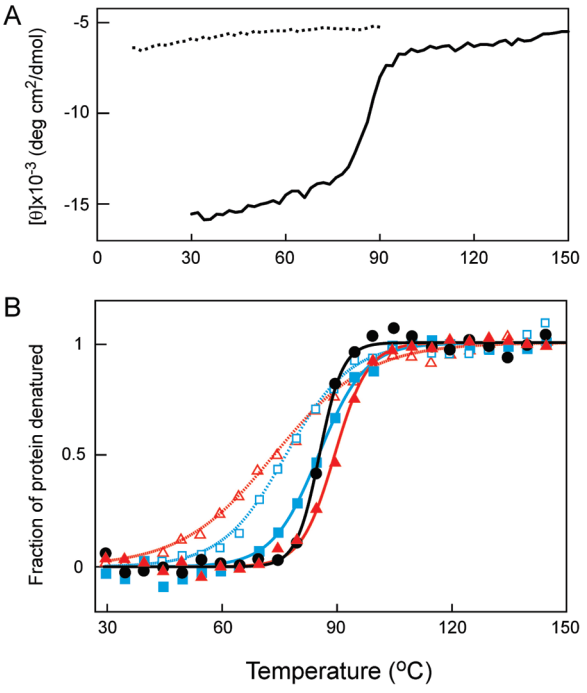

Figure 3. Thermal denaturation of the holo and apo forms of cytochromes *c*. (A) The raw CD data at 222 nm for the holo (solid line) and apo (dotted line) PA c_{551} wild-type proteins were obtained as a function of temperature. (B) The normalized fractions of protein denatured are plotted as a function of temperature, and the fitting curve for each experiment is also shown. The normalized raw data for the holocytochromes *c* are indicated by closed symbols and those for the apocytochromes *c* by open symbols, with 5 °C intervals. The fitting curves for the holocytochromes *c* are indicated by solid lines and those for the apocytochromes *c* by dotted lines. The data for the PA c_{551} wild type (black symbols and line), PA-nh (red symbols and line), and PA-nh/eh (blue symbols and line) are shown.

protein denaturation of the PA-nh variant, as exemplified by its ΔS_m value being smaller than that of the holo PA c_{551} wild type (Table 2). Furthermore, the ΔH_m value of the holo PA-nh/eh variant was smaller than that of holo PA-nh (Table 2). This enthalpic disadvantage of holo PA-nh/eh, compared with holo PA-nh, indicates that the residues forming the extra helix of AA c_{555} result in further loss of interactions in the holo PA-nh/eh variant.

Effects of Mutations on the Thermal Stability of Apocytochromes *c*. In order to thermodynamically elucidate the effects of mutations on the protein structures of the PA c_{551} wild type, PA-nh, and PA-nh/eh in their apo states, thermal denaturation experiments were carried out. The apo PA c_{551} wild type exhibited no transition with the temperature increase from 10 to 90 °C (Figure 3A); thus we could not determine its thermodynamic parameters (Table 3). In contrast, the apo forms of the PA-nh and PA-nh/eh variants became cooperatively denatured from 30 to 150 °C (Figure 3B), apparently indicating that protein denaturation proceeds in a two-state transition manner, the T_m values being 73.7 °C for apo PA-nh and 77.3 °C for apo PA-nh/eh (Table 3).

Judging from the measurable values for thermodynamic parameters (T_m, ΔH_m, and ΔS_m) of the apo forms of the PA-nh and PA-nh/eh variants (Table 3), their structural stability seems to be enhanced by the mutations as compared with the case of the apo PA c_{551} wild type. It is obvious that the apo PA-nh and PA-nh/eh variants were stabilized to the same extent as in the case of naturally occurring and thermally stable apo AA c_{555} in terms of the T_m values. In addition, the ΔH_m value of the apo PA-nh/eh variant was greater than that of apo PA-nh. The more favorable enthalpy for apo PA-nh/eh than for apo PA-nh is probably due to the formation of an additional helix, which is consistent with the results of static CD analysis (Figure 2).

Effects of Heme on the Thermal Stability of Cytochormes *c*. The above thermal stability analysis provided us with a chance to examine the effects of heme on the stability of PA-nh and PA-nh/eh, as evidenced by the $\Delta\Delta G_{heme}$ values, representing the difference in free energy change during protein denaturation between the apo- and holoproteins. The $\Delta\Delta G_{heme}$ values were estimated to be −13.3 kJ/mol for PA-nh and −4.6 kJ/mol for PA-nh/eh (Table 4), indicating the thermodynamic advantage of a holocytochrome *c* with covalently bound heme, as observed by others.[25,28−30]

As the $\Delta\Delta G_{heme}$ value can only be estimated when the thermodynamic parameters of both the apo and holo forms are available, the equivalent value for AA c_{555} is listed in Table 4 as an example of that of a naturally occurring cytochrome *c*. The $\Delta\Delta G_{heme}$ value of AA c_{555} was estimated to be −74.3 kJ/mol, which was 6−16-fold those of the PA-nh and PA-nh/eh variants, respectively. These results indicate that the naturally occurring AA c_{555} protein exhibits a far greater thermodynamic advantage with the covalently bound heme than the PA-nh and PA-nh/eh

Table 2. Thermodynamic Parameters of Holocytochromes *c*

protein	T_m (°C)	ΔT_m(mut-wt) (°C)	ΔH_m (kJ/mol)	ΔS_m (kJ mol^{-1} K^{-1})	$\Delta\Delta G_{mut}$ (kJ/mol)
PA c_{551} wild type	85.7 ± 0.6	0	346.2 ± 13	0.96 ± 0.03	0
PA-nh	90.5 ± 0.1	4.8	286.3 ± 12.5	0.79 ± 0.03	4.6
PA-nh/eh	86.5 ± 0.6	0.8	179.5 ± 10.9	0.5 ± 0.03	0.8
AA c_{555}[a]	129.7 ± 0.1	NA[b]	537.0 ± 18.4	1.33 ± 0.05	NA[b]

[a] For comparison with a naturally occurring cytochrome *c*, the thermodynamic parameters of holo AA c_{555} calculated from the data in our previous paper[6] are also listed. These data are also used in Table 4 below. [b] Not applicable.

Table 3. Thermodynamic Parameters of Apocytochromes *c*

protein	T_m (°C)	ΔH_m (kJ/mol)	ΔS_m (kJ mol^{-1} K^{-1})
PA c_{551} wild type	ND[b]	ND[b]	ND[b]
PA-nh	73.7 ± 0.7	79.0 ± 5.5	0.23 ± 0.02
PA-nh/eh	77.3 ± 1.0	120.1 ± 3.5	0.34 ± 0.01
AA c_{555}[a]	73.8 ± 0.2	95.4 ± 2.1	0.27 ± 0.01

[a] For comparison with a naturally occurring cytochrome *c*, the thermodynamic parameters of apo AA c_{555} calculated from the data in our previous paper[6] are also listed. These data are also used in Table 4 below. [b] Not determined.

Table 4. Effects of Covalent Heme Binding

protein	ΔT_m(apo-holo) (°C)	$\Delta\Delta G_{heme}$ (kJ/mol)
PA-nh	−16.8	−13.3
PA-nh/eh	−9.2	−4.6
AA c_{555}[a]	−55.9	−74.3

[a] For comparison with a naturally occurring cytochrome *c*, the calculated values for the AA c_{555} protein are listed using data from Tables 2 and 3.

variants. In these engineered variants, some introduced residues may directly and/or indirectly cause steric hindrance in the holo.

DISCUSSION

To date, a large number of experiments have been carried out to elucidate the folding mechanism for holocytochromes *c* with covalently bound heme.[31−36] The folding of cytochromes *c* on binding of heme or lipid micelles to the apoprotein has also been shown.[3−5,37−39] Cytochrome *c* folding is supposed to require heme binding. Judging from the results of structural analysis of holocytochromes *c*, the heme interacts with hydrophobic residues spatially distributed in the protein interior.[35,40,41] Hence, hydrophobic interactions between the heme and hydrophobic residues are generally believed to be one of the essential factors for cytochrome *c* folding.

In contrast to the research progress regarding cytochrome *c* folding with the aid of heme, the folding ability of apocytochromes *c* has rarely been examined. There have been a few reports demonstrating apocytochrome *c* folding, but only under harsh solvent conditions, i.e., at extremely low pH and/or high ionic strength.[42,43] To our knowledge, AA c_{555} represents the first and only case of an apocytochrome *c* folded to the same extent as its holo form in terms of the helix content under nearly physiological solvent conditions.[6]

In this study, the three-dimensional structures of the holo forms of AA c_{555} and PA c_{551} were compared. These cytochromes *c* are structurally homologous in their holo states, but apo PA c_{551} is unfolded, unlike apo AA c_{555}. Here we speculate that nine hydrophobic residues and the extra helix of AA c_{555}, which are absent in the PA c_{551} structure, are responsible for the folding ability of apo AA c_{555}. To verify this speculation, the PA-nh variant carrying the nine hydrophobic residues of AA c_{555} and the PA-nh/eh variant carrying the amino acid residues forming the extra helix plus the nine hydrophobic residues of AA c_{555} were examined as to folding ability in their apo states. In contrast to the apo PA c_{551} wild type, the apo PA-nh and PA-nh/eh variants exhibited a helical structure at neutral pH and low ionic strength. In addition, thermal denaturation analysis showed that the apo PA-nh and PA-nh/eh variants are thermodynamically far more stabilized than the apo PA c_{551} wild type. These results together indicate that the nine hydrophobic residues introduced into these variants are enough to confer the folding ability on the apo states and that the amino acid residues forming the extra helix of AA c_{555}, which were introduced in the PA-nh/eh, are not necessarily required for the apo folding.

What are the roles of the nine hydrophobic residues during the protein folding in the apo PA-nh and PA-nh/eh variants? As these residues, originally found in AA c_{555}, are more hydrophobic than the respective ones in the PA c_{551} wild type, these residues form a tightly hydrophobic core in the interior of holo AA c_{555}. It is likely that the introduction of these residues into the apo PA c_{551} wild type results in the formation of hydrophobic interactions, as found in holo AA c_{555}. This has been proved in this study by the thermodynamic effects on the apoprotein stability.

In contrast, the nine hydrophobic residues cause rearrangement of the heme vicinity in the holo PA-nh and PA-nh/eh variants, suggesting that the introduced residues cause steric hindrance with the heme. Probably the atomic geometry in the protein interior is more harmonious in the naturally occurring holo AA c_{555} protein than in the holo PA-nh and PA-nh/eh variants. Currently ongoing structural studies on the PA-nh and PA-nh/eh variants will offer insights as to the interactions between the heme and polypeptide.

Hemoproteins, proteins with heme(s) functioning as cofactor(s), are classified into two groups in terms of protein folding. Cytochromes *c* represent one group, which is characterized by an unfolded structure in the apo state. The other group includes *E. coli* periplasmic cytochrome b_{562}, a four-helix bundle protein with noncovalent-bound heme, in which a large portion of the protein is autonomously folded even in the apo state.[44] AA c_{555} is an exceptional cytochrome *c* in that it is folded in the apo state,[6] and its nine hydrophobic residues were introduced into an orthodox cytochrome *c*, PA c_{551}, in this study. Our present results demonstrate that PA c_{551} represents the first example of conversion of an intrinsically unfolded apocytochrome *c* into an autonomously folded one, which was revealed by means of a protein engineering method without heme. Heme is generally considered as a trigger of apocytochrome *c* folding through the formation of hydrophobic interactions with the protein. Our understanding of hemoprotein classification from the aspect of folding with heme should be amended.

AUTHOR INFORMATION

Corresponding Author

*Tel/Fax: +81 82 424 7924. E-mail: sambongi@hiroshima-u.ac.jp.

Funding Sources

This work was in part supported by Grants-in-Aid for Scientific Research on Innovative Areas (No. 20118005) from the Ministry of Education, Culture, Sports, Science, and Technology of Japan.

ACKNOWLEDGMENT

We are grateful to Professor Y. Yamamoto, Dr. H. Tai, and Dr. S. Mikami for the CV measurements and useful comments.

ABBREVIATIONS

AA c_{555}, *Aquifex aeolicus* cytochrome c_{555}; CD, circular dichroism; CV, cyclic voltammetry; DTT, dithiothreitol; HT c_{552}, *Hydrogenobacter thermophilus* cytochrome c_{552}; PA c_{551}, *Pseudomonas aeruginosa* cytochrome c_{551}; PA-nh, *Pseudomonas aeruginosa* cytochrome c_{551} with mutations of nine hydrophobic amino acid residues; PA-nh/eh, *Pseudomonas aeruginosa* cytochrome c_{551} with mutations of nine hydrophobic amino acid residues and the amino acid residues forming the extra helix of AA c_{555}; PCR, polymerase chain reaction; SDS−PAGE, sodium dodecyl sulfate−polyacrylamide gel electrophoresis; SHE, standard hydrogen electrode.

REFERENCES

(1) Stellwagen, E., Rysavy, R., and Babul, G. (1972) The conformation of horse heart apocytochrome *c*. *J. Biol. Chem. 247*, 8074–8077.

(2) Fisher, W. R., Taniuchi, H., and Anfinsen, C. B. (1973) On the role of heme in the formation of the structure of cytochrome *c*. *J. Biol. Chem. 248*, 3188–3195.

(3) Dumont, M. E., Corin, A. F., and Campbell, G. A. (1994) Noncovalent binding of heme induces a compact apocytochrome *c* structure. *Biochemistry 33*, 7368–7378.

(4) Daltrop, O., Allen, J. W., Willis, A. C., and Ferguson, S. J. (2002) *In vitro* formation of a *c*-type cytochrome. *Proc. Natl. Acad. Sci. U.S.A. 99*, 7872–7876.

(5) Daltrop, O., and Ferguson, S. J. (2003) Cytochrome c maturation. The *in vitro* reactions of horse heart apocytochrome *c* and *Paracoccus dentrificans* apocytochrome c_{550} with heme. *J. Biol. Chem. 278*, 4404–4409.

(6) Yamanaka, M., Mita, H., Yamamoto, Y., and Sambongi, Y. (2009) Heme is not required for *Aquifex aeolicus* cytochrome c_{555} polypeptide folding. *Biosci., Biotechnol., Biochem. 73*, 2022–2025.

(7) Wain, R., Pertinhez, T. A., Tomlinson, E. J., Hong, L., Dobson, C. M., Ferguson, S. J., and Smith, L. J. (2001) The cytochrome *c* fold can be attained from a compact apo state by occupancy of a nascent heme binding site. *J. Biol. Chem. 276*, 45813–45817.

(8) Obuchi, M., Kawahara, K., Motooka, D., Nakamura, S., Yamanaka, M., Takeda, T., Uchiyama, S., Kobayashi, Y., Ohkubo, T., and Sambongi, Y. (2009) Hyperstability and crystal structure of cytochrome c_{555} from hyperthermophilic *Aquifex aeolicus*. *Acta Crystallogr., Sect. D: Biol. Crystallogr. 65*, 804–813.

(9) DeLano, W. L. (2002) *The PyMOL Molecular Graphics System* (http://pymol.sourceforge.net).

(10) Hussain, H., Grove, J., Griffiths, L., Busby, S., and Cole, J. (1994) A seven-gene operon essential for formate-dependent nitrite reduction to ammonia by enteric bacteria. *Mol. Microbiol. 12*, 153–163.

(11) Hasegawa, J., Shimahara, H., Mizutani, M., Uchiyama, S., Arai, H., Ishii, M., Kobayashi, Y., Ferguson, S. J., Sambongi, Y., and Igarashi, Y. (1999) Stabilization of *Pseudomonas aeruginosa* cytochrome c_{551} by systematic amino acid substitutions based on the structure of thermophilic *Hydrogenobacter thermophilus* cytochrome c_{552}. *J. Biol. Chem. 274*, 37533–37537.

(12) Arslan, E., Schulz, H., Zufferey, R., Künzler, P., and Thöny-Meyer, L. (1998) Overproduction of the *Bradyrhizobium japonicum c*-type cytochrome subunits of the cbb3 oxidase in *Escherichia coli*. *Biochem. Biophys. Res. Commun. 251*, 744–777.

(13) Sambongi, Y., Stoll, R., and Ferguson, S. J. (1996) Alteration of haem-attachment and signal-cleavage sites for *Paracoccus denitrificans* cytochrome c_{550} probe pathway of *c*-type cytochrome biogenesis in *Escherichia coli*. *Mol. Microbiol. 19*, 1193–1204.

(14) Scopes, R. K. (1974) Measurement of protein by spectrophotometry at 205 nm. *Anal. Biochem. 59*, 277–282.

(15) Bartsch, R. G. (1971) Cytochromes: Bacterial. *Methods Enzymol. 23*, 344–363.

(16) Takayama, S. J., Mikami, S., Terui, N., Mita, H., Hasegawa, J., Sambongi, Y., and Yamamoto, Y. (2005) Control of the redox potential of *Pseudomonas aeruginosa* cytochrome c_{551} through the Fe-Met coordination bond strength and pK_a of a buried heme propionic acid side chain. *Biochemistry 44*, 5488–5494.

(17) Takeda, T., Sonoyama, T., Takayama, S. J., Mita, H., Yamamoto, Y., and Sambongi, Y. (2009) Correlation between the stability and redox potential of three homologous cytochromes *c* from two thermophiles and one mesophile. *Biosci., Biotechnol., Biochem. 73*, 366–371.

(18) Ohshima, A., Uchiyama, S., Nakano, H., Yoshida, T., Ohkubo, T., and Kobayashi, Y. (2003) CD measurement of aqueous protein solution at high temperature up to 180°C—Thermodynamic analysis of thermophilic protein by pressure-proof cell compartment. *Lett. Pept. Sci. 10*, 539–543.

(19) Uchiyama, S., Ohshima, A., Nakamura, S., Hasegawa, J., Terui, N., Takayama, S. J., Yamamoto, Y., Sambongi, Y., and Kobayashi, Y. (2004) Complete thermal-unfolding profiles of oxidized and reduced cytochromes *c*. *J. Am. Chem. Soc. 126*, 14684–14685.

(20) Oikawa, K., Nakamura, S., Sonoyama, T., Ohshima, A., Kobayashi, Y., Takayama, S. J., Yamamoto, Y., Uchiyama, S., Hasegawa, J., and Sambongi, Y. (2005) Five amino acid residues responsible for the high stability of *Hydrogenobacter thermophilus* cytochrome c_{552}. *J. Biol. Chem. 280*, 5527–5532.

(21) Becktel, W. J., and Schellman, J. A. (1987) Protein stability curves. *Biopolymers 26*, 1859–1877.

(22) Monera, O. D., Sereda, T. J., Zhou, N. E., Kay, C. M., and Hodges, R. S. (1995) Relationship of sidechain hydrophobicity and α-helical propensity on the stability of the single-stranded amphipathic α-helix. *J. Pept. Sci. 1*, 319–329.

(23) Kauzmann, W. (1959) Some factors in the interpretation of protein denaturation. *Adv. Protein Chem. 14*, 1–63.

(24) Barker, P. D., Nerou, E. P., Freund, S. M., and Fearnley, I. M. (1995) Conversion of cytochrome b_{562} to *c*-type cytochromes. *Biochemistry 34*, 15191–15203.

(25) Tomlinson, E. J., and Ferguson, S. J. (2000) Loss of either of the two heme-binding cysteines from a class I *c*-type cytochrome has a surprisingly small effect on physicochemical properties. *J. Biol. Chem. 275*, 32530–32534.

(26) Andrade, M. A., Chacón, P., Merelo, J. J., and Morán, F. (1993) Evaluation of secondary structure of proteins from UV circular dichroism using an unsupervised learning neural network. *Protein Eng. 6*, 383–390.

(27) Merelo, J. J., Andrade, M. A., Prieto, A., and Morán, F. (1994) Proteinotopic feature maps. *Neurocomputing 6*, 443–454.

(28) Arnesano, F., Banci, L., Bertini, I., Ciofi-Baffoni, S., Woodyear, T. L., Johnson, C. M., and Barker, P. D. (2000) Structural consequences of *b*- to *c*-type heme conversion in oxidized *Escherichia coli* cytochrome b_{562}. *Biochemistry 39*, 1499–1514.

(29) Faraone-Mennella, J., Tezcan, F. A., Gray, H. B., and Winkler, J. R. (2006) Stability and folding kinetics of structurally characterized cytochrome *c*-b_{562}. *Biochemistry 45*, 10504–10511.

(30) Tomlinson, E. J., and Ferguson, S. J. (2000) Conversion of a *c* type cytochrome to a *b* type that spontaneously forms in vitro from apo protein and heme: Implications for *c* type cytochrome biogenesis and folding. *Proc. Natl. Acad. Sci. U.S.A. 97*, 5156–5160.

(31) Goto, Y., Takahashi, N., and Fink, A. L. (1990) Mechanism of acid-induced folding of proteins. *Biochemistry 29*, 3480–3488.

(32) Colón, W., Elöve, G. A., Wakem, L. P., Sherman, F., and Roder, H. (1996) Side chain packing of the N- and C-terminal helices plays a critical role in the kinetics of cytochrome *c* folding. *Biochemistry 35*, 5538–5549.

(33) Brunori, M., Bigotti, M. G., Cutruzzolà, F., Gianni, S., and Travaglini-Allocatelli, C. (2003) Cytochrome c_{551} as a model system for protein folding. *Biophys. Chem. 100*, 409–419.

(34) Travaglini-Allocatelli, C., Gianni, S., and Brunori, M. (2004) A common folding mechanism in the cytochrome *c* family. *Trends Biochem. Sci. 29*, 535–541.

(35) Travaglini-Allocatelli, C., Gianni, S., Dubey, V. K., Borgia, A., Di Matteo, A., Bonivento, D., Cutruzzolà, F., Bren, K. L., and Brunori, M. (2005) An obligatory intermediate in the folding pathway of cytochrome c_{552} from *Hydrogenobacter thermophilus*. *J. Biol. Chem. 280*, 25729–25734.

(36) Kinoshita, M., Kamagata, K., Maeda, A., Goto, Y., Komatsuzaki, T., and Takahashi, S. (2007) Development of a technique for the investigation of folding dynamics of single proteins for extended time periods. *Proc. Natl. Acad. Sci. U.S.A. 104*, 10453–10458.

(37) Bryson, E. A., Rankin, S. E., Carey, M., Watts, A., and Pinheiro, T. J. (1999) Folding of apocytochrome *c* in lipid micelles: Formation of alpha-helix precedes membrane insertion. *Biochemistry 38*, 9758–9767.

(38) Rankin, S. E., Watts, A., and Pinheiro, T. J. (1998) Electrostatic and hydrophobic contributions to the folding mechanism of apocytochrome *c* driven by the interaction with lipid. *Biochemistry 37*, 12588 12595.

(39) Rankin, S. E., Watts, A., Roder, H., and Pinheiro, T. J. (1999) Folding of apocytochrome *c* induced by the interaction with negatively charged lipid micelles proceeds via a collapsed intermediate state. *Protein Sci. 8*, 381–393.

(40) Matsuura, Y., Takano, T., and Dickerson, R. E. (1982) Structure of cytochrome c_{551} from *Pseudomonas aeruginosa* refined at 1.6 Å resolution and comparison of the two redox forms. *J. Mol. Biol. 156*, 389–409.

(41) Bushnell, G. W., Louie, G. V., and Brayer, G. D. (1990) High-resolution three-dimensional structure of horse heart cytochrome *c*. *J. Mol. Biol. 214*, 585–595.

(42) Hamada, D., Hoshino, M., Kataoka, M., Fink, A. L, and Goto, Y. (1993) Intermediate conformational states of apocytochrome *c*. *Biochemistry 32*, 10351–10358.

(43) Borgia, A., Gianni, S., Brunori, M., and Travaglini-Allocatelli, C. (2008) Fast folding kinetics and stabilization of apo-cytochrome *c*. *FEBS Lett. 582*, 1003–1007.

(44) Feng, Y., Sliger, S. G., and Wand, A. J. (1994) Solution structure of apocytochrome b_{562}. *Nat. Struct. Biol. 1*, 30–35.